Ultrasonic Scattering in Deformed Media and the Effects on Strain Imaging

Michael F. Insana[1], Tim Hall[2], Pawan Chaturvedi[3]
[1]Biomedical Engineering, University of California, Davis, CA 95616
[2] Radiology, KUMC, Kansas City, KS 66160
[3] Sprint Corporation, Overland Park, KS 66210

Abstract— **Acoustic properties of tissue-like media with stiff and soft scatterers were measured as a function of compressive strain up to 40%. Uniaxial strain measurements were analyzed to test the assumption that local properties of wave propagation and scattering are invariant under deformation. We found that echo spectra of gel media with soft scatterers varied significantly and predictably during compression. Specifically, centroids of Gaussian echo spectra were shifted to higher frequencies in proportion to the compressive strain applied up to 10%, and increased monotonically up to 40% at a rate depending on the scatterer size. The results explain why there is often more echo decorrelation produced in tissues than in commonly used graphite-gelatin test phantoms.**

I. Introduction

THE motivation for our study originated during early elasticity imaging experiments designed to explore relationships between large- and small-scale viscoelastic properties of tissue-like media [1]. Echo correlation provides a reliable method for tracking object motion only if the acoustic properties are invariant under deformation. Specifically, the microscopic distribution of bulk moduli that dominates scattering properties in soft tissues must be independent of the macroscopic distribution of shear moduli that determines the appearance of tissue strain images. Coupling the two moduli leads to a decorrelation between pre- and post-deformation echoes that cannot be recovered by signal processing, thus imposing a fundamental limitation in strain estimation via echo correlation.

This paper summarizes a series of experiments involving two classes of materials originally developed by Madsen et al [3] as ultrasound phantoms for studying acoustic properties of biological tissues. Type I materials are glass-sphere-in-gelatin *suspensions* and type II materials are oil-droplet-in-gelatin *dispersions*. The diameter ranges of glass microspheres in the type I samples are either 35 - 75 μm or 150 - 180 μm. All glass microspheres are randomly positioned and much stiffer than the surrounding gelatin. Type II materials contain oil spheres dispersed randomly throughout the gelatin. The mean oil sphere diameter varies in different samples between 20 and 400 μm. At room temperature, the oils are liquids, similar to lipid at body temperature, and therefore much softer than the surrounding gelatin.

We measured speeds of sound, attenuation coefficients and backscattered echo spectra for each sample up to 10 MHz and for known, uniaxial strains between 0 and 40% to observe changes in these acoustic properties (Fig 1). Although compressive strains ϵ' were *applied* uniaxially to samples along the $-x_3$ direction, *induced* strains were three dimensional and related to ϵ' via the measurement geometry and Poisson's ratio ν. For these nearly incompressible ($\nu \simeq 0.5$) cylindrical samples, parallel-plate compressor geometry, and full-slip boundary conditions, sample volume is conserved and $\epsilon_{11} = \epsilon_{22} \simeq 1/\sqrt{\epsilon'}$, $\epsilon_{33} \simeq \epsilon'$. The results below indicate the reliability of echo tracking in a broad range of deformations for tissue-like media, and suggest a new method for identifying the anatomical sources of bioacoustic scattering.

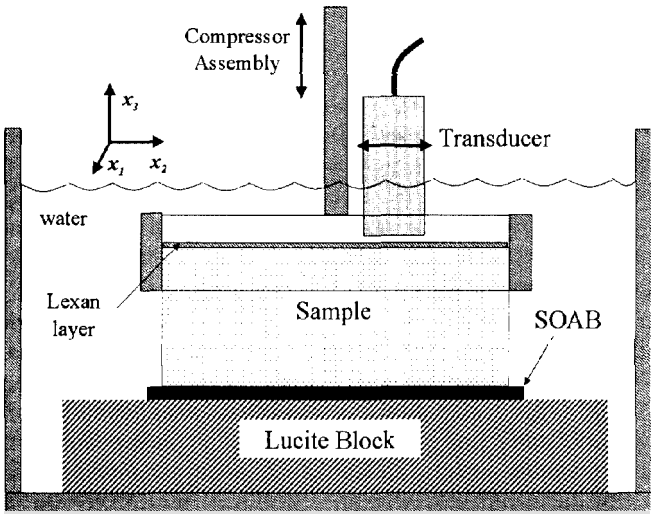

Fig. 1. Apparatus for measuring the acoustic properties of deformed samples.

II. Materials and Methods

Type I Materials [4]. One-hundred twenty grams of animal hide gelatin were mixed into each liter of a 6% n-propanol-in-water solution at room temperature. The mixture was placed in a vacuum for a few minutes to remove gases. The beaker of dissolved, degassed gelatin was then heated to 45°C in a water bath about 90 minutes until it became translucent. The clear gelatin solution was removed from the heat, glass microspheres (Table 1) were added and thoroughly mixed with a spoon, and the beaker was

This study was supported in part by a grant from NIH CA82497.
E-mail: mfinsana@ucdavis.edu.

cooled to 30°C while stirring. The liquid glass-gel mixture was poured into a cylindrical mold, sealed, and rotated overnight. Congealed samples were removed from the molds and stored at room temperature.

Type II Materials [3], [4]. More of the clear gelatin solution described above was heated in a water bath to 70°C. Instead of glass microspheres, 250 ml of an oil were emulsified into each liter of liquid gelatin by vigorous mixing with a spoon. The different types of oils used in this study are listed in Table 2. Care was taken to prevent introducing air while mixing. The emulsion was cooled to 30°C before being poured into the cylindrical molds and rotated in room air overnight. After congealing and removal from its mold, an inspection microscope was used to measure the average diameter of oil drops visible from the surface of the colloid, now a dispersion.

Acoustic measurements. Measurements were made in distilled/degassed water at room temperature with the apparatus of Fig 1. Transducers had one 19 mm-diameter, f/2.8, circular PZT element. Test samples were deformed by uniformly displacing the top surface of the sample downward a known amount while holding the bottom surface fixed.

A pulse-echo variation on the standard through-transmission substitution technique described by Madsen et al. [3] was used to measure sound speed and attenuation. Twenty-cycle sinusoidal pressure bursts were reflected from a 5-cm-thick Lucite block at normal incidence and with the sound-absorbing (SOAB) layer removed (Fig 1). The transducer-reflector distance remained unchanged during sample compression and was approximately equal to the radius of curvature of the transducer; i.e., the transducer and compressor moved independently. We recorded measurements of echo phase ϕ and amplitude A near the center of the burst from a digital oscilloscope display. $L = 10$ independent measurement pairs (A_ℓ, ϕ_ℓ), $1 \le \ell \le L$, were obtained after scanning the transducer at 2 mm lateral increments with the sample in place. One reference measurement pair (A_0, ϕ_0) was recorded with the sample removed. Wave properties in the latter case are determined entirely by the distilled water, but, in both situations, the thin Lexan layer used to compress the sample uniformly remained in place.

The substitution technique involves an expression of the speed of sound in a sample, $c(\epsilon', T)$ [m/s], as a function of the applied strain ϵ', measurement temperature T [°C], speed of sound in water $c_0(T)$ [m/s], sample thickness $x(\epsilon')$ [m], and mean phase shift introduced by placing the sample in the sound beam $\Delta\phi$ [s] $= \left(\sum_{\ell=1}^{L} \phi_\ell\right)/L - \phi_0$. Writing $\Delta\phi(\epsilon', T) = 2x(\epsilon')\,(1/c(\epsilon', T) - 1/c_0(T))$ and rearranging terms, we find that

$$c(\epsilon', T) \;=\; \frac{2x(\epsilon')c_0(T)}{2x(\epsilon') + c_0(T)\Delta\phi(\epsilon', T)} \,. \qquad (1)$$

Attenuation coefficients, $\alpha(f, \epsilon', T)$, at frequency f [MHz] were found from the ratio of peak-to-peak burst amplitudes with $\left(A = \left(\sum_{\ell=1}^{L} A_\ell\right)/L\right)$ and without (A_0) the sample in place and sample thickness x via

$$\alpha(f, \epsilon', T) \;=\; \frac{10}{x(\epsilon')} \log_{10} \frac{A(f, \epsilon', T)}{A_0(f, T)} \,. \qquad (2)$$

Castor oil was used as a standard sample to calibrate attenuation estimates [3]. Large-amplitude sinusoids were transmitted, yet the amplitude was subject to the constraints of linearity and agreement (±3%) with published values for attenuation in castor oil: $0.834\, f^{5/3}$ [dB/cm] at 20°C.

Following measurements of sound speed and attenuation, echo spectra were recorded. We digitized 10.24 μs echo time series generated by backscatter of broad-band pulses within a sample. The transmitted pulse duration was approximately 2 cycles, producing a -6 dB bandwidth of 60% of the peak frequency for pulses reflected from a Lucite surface in water at 20°C . L was increased to 25 waveforms, each digitized at 5×10^7 samples/s to give $N = 512$ points per waveform. Adjusting the transducer-sample distance, we placed the center of the time series at the radius of curvature of the transducer. A SOAB layer was used as shown in Fig 1 to reduce reverberations.

The magnitude of the discrete Fourier transform $|G[k]|$, $0 \le k \le N/2$, was computed using a fast Fourier transform algorithm. From the set of recorded time series, $g_{\ell,\epsilon}[n]$, $0 \le n \le N-1$, at each applied strain ϵ', we estimated the discrete frequency spectrum

$$|G_\epsilon[k]| = \frac{1}{L} \sum_{\ell=1}^{L} \left| \sum_{n=0}^{N-1} g_{\ell,\epsilon}[n]\, e^{-i2\pi kn/N} \right| \,. \qquad (3)$$

Echo spectra shown in the Results section below describe a shift in the peak for $|G_\epsilon[k]|$ with increasing ϵ'. We summarized changes in echo spectra by a scalar value obtained from estimates of the normalized first moment or spectral *centroid* [5],

$$f_c(\epsilon') \;=\; \Delta f \frac{\sum_{k=0}^{N/2} k\,|G_\epsilon[k]|}{\sum_{k=0}^{N/2} |G_\epsilon[k]|} \,, \qquad \Delta f = \frac{1}{NT} \,, \qquad (4)$$

where T is the sampling interval, in this case 20 ns. The centroid defined above gives the center-of-mass frequency in MHz for the magnitude of the mean echo spectrum. This quantity indicates any monotonic weighting of spectral values, such as those expected for a change in scatterer size with ϵ'.

Centroid predictions. It is reasonable to assume that the local stress field induced by an applied strain will deform soft scatterers in the same manner as the surrounding gelatin matrix. Therefore we hypothesize that changes in the ultrasonic echo spectrum can be predicted if we understand how backscatter from oblate spherical oil droplets varies with spherical eccentricity, i.e., ratio of minor to major axes, $r(\epsilon')$ (Fig 3). Fortunately an expression for the incoherent backscattered pressure amplitude versus $r(\epsilon')$ for a random distribution of acoustically-soft oblate spheroids is known [6]. Assuming linear superposition of frequencies and single scatter from an incident plane-wave pressure field over the dimensions of the oil drop, we integrated

the exact numerical solution for the complex pressure field of a single spheroid as a function of vector position $\mathbf{x}$, $V_s'(f, \mathbf{x}, \epsilon')$, over the transducer aperture. Multiplying the integral by the average number of scatterers in a pulse volume we found $V_s(f, \epsilon')$. That result was multiplied by a Gaussian system response, $H(f)$, computed for the same peak frequency and bandwidth as the transducers used experimentally to predict the magnitude of the echo spectrum:

$$|\tilde{G}_\epsilon[k]| = |H(k\Delta f)V_s(k\Delta f, \epsilon')| \ , \qquad f = k\Delta f \ . \qquad (5)$$

Finally, the predicted spectral centroid, $\tilde{f}_c(\epsilon')$, was computed from Eq (4), where $|\tilde{G}_\epsilon[k]|$ replaced $|G_\epsilon[k]|$.

III. Results

Sound speed was measured at 2.5 MHz and ϵ' up to 20% for three oil-in-gel dispersion samples and both glass-in-gel suspension samples (Tables 1 and 2).[1] No significant change in speed with compression was observed. We conclude that sound speed is invariant under compressive strain, i.e., $c(\epsilon', T) = c(T)$.

We also examined the relative change in attenuation coefficient for four oil-in-gel dispersions and both glass-in-gel suspensions up to 20% compression. There was a slight increase in attenuation with compression for the dispersions: the regression lines gave $\alpha/\alpha_0 = 0.0076\,C + 0.993$ at 2.5 MHz and $\alpha/\alpha_0 = 0.0025\,C + 0.991$ at 5.0 MHz, where $C = 100\epsilon'$ is percent compression. Nevertheless, statistical tests showed neither slope varied significantly from zero. Therefore $\alpha(f, \epsilon', T) \simeq \alpha(f, T)$, and no attenuation adjustments to echo spectra were deemed necessary.

There was a significant change in the centroid of the echo spectra with ϵ' for the dispersions but not the suspensions. The spectral shift is clearly visible in the measured centroid shifts plotted in Fig 2; $\Delta f_c = f_c(\epsilon') - \bar{f}_c(0)$, where $\bar{f}(0)$is the average value for all six uncompressed samples listed in Tables 1 and 2. Note that $f_c(0)$ is determined primarily by the response of the ultrasound system, so centroids measured for each undeformed sample are similar. For $0 \le \epsilon' \le 0.3$, the centroid shifts measured for the two glass-in-gel samples were zero; stiff scatterers are spatially reoriented but not individually deformed. The number density of scatterers remains constant with ϵ' because the gelatin is incompressible. However, liquid oil scatterers, being softer than the gel, easily deform with the gelatin. The change in oil drop shape increases scattering preferentially at high frequencies, thus shifting the centroid to larger values.

Measured values of Δf_c for oil-in-gel samples are accurately predicted by Eq (5), as seen by the lines in Fig 2. We see larger centroid shifts for smaller oil drops at higher compressions. We examined the surface of several oil-in-gel samples under an inspection microscope and found that the

[1]The acoustic properties listed in Tables 1 and 2 are for uncompressed samples ($\epsilon' = 0$). Averaging attenuation coefficients for corn, motor, and peanut oils, we find the following power law describes the frequency dependence between 2.5 and 10.0 MHz:
$\alpha(f) = 0.21\,f^{1.72}$, $r = 0.999$.

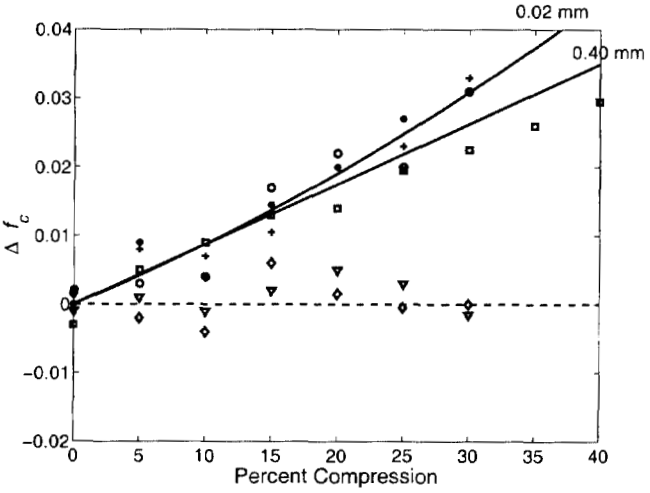

Fig. 2. Measured (pts) and predicted (lines) values for changes in echo centroid with uniaxial compression. ◇ sample 1, ▽ sample 2, (•, +) sample 3, ○ sample 5, □ sample 6. Upper and lower solid lines are predictions for 0.02 mm and 0.40 mm oil spheres, respectively.

two corn oil (samples 3 and 3′) and the peanut oil (sample 5) samples had the smallest oil-drop diameter, roughly 20 μm. The average diameter of mineral oil drops was much larger, roughly 400 μm. Oil-drop size appears to be determined by oil viscosity and mixing time. The agreement among measured and predicted data in Fig 2 leads us to conclude that deformation of scatterers softer than the background produces measurable and predictable changes in the *mean* echo spectrum not observed with scatterers much stiffer than the background.

Samples were found to fracture between $30\% < C < 40\%$. Therefore c, α measurements were limited to $C < 20\%$ to ensure sample integrity for scattering measurements. Echo spectra were acquired on each sample at 5% increments until evidence of fracture became evident.

IV. Discussion

Scattering in most biological tissues is believed to be a small percentage of the total attenuation. Absorption mechanisms dominate propagational losses. Based on more than a decade of experimentation with phantoms, our impressions are that scattering equals or exceeds absorptive losses in the glass-in-gel samples and absorption dominates attenuation in the oil-in-gel dispersion samples. However, measurements of total scattering cross sections are needed to make that determination, and those measurements have not been made. Given these observations, it is not surprising that the mean echo spectrum in compressed dispersions can change without significantly affecting attenuation coefficients.

The observed spectral variance suggests that echo waveforms from lipid-filled biological media, such as breast tissue, will decorrelate when strained. Figure 2 shows that Δf_c is directly proportional to ϵ' with unit slope for compressions up to 10%. Greater than 10%, the magnitude of

the centroid shift depends on scatterer diameter, increasing faster for Rayleigh scatterers than Mie scatterers. This source of waveform decorrelation, which has not been discussed in the literature previously, could pose fundamental limitations for elasticity imaging of tissues with lipid-filled scattering sites.

We anticipated the effects of simple scaling strains on the frequency response of scattering from random *point* targets, and suggested a pulse-shaping method to mitigate waveform decorrelation [1]. Pulse shaping would be helpful for strain estimation in the glass-in-gel samples. However, deformation of finite-size scatterers, as described in this report, further decorrelates echo waveforms in a manner that cannot be anticipated or compensated for in an individual spectrum, e.g., that from a single time series. Scatterer deformation is an irreversible source of echo decorrelation. Strain imaging algorithms that work well in simulation or using phantom data, often perform at reduced levels in tissues, in the sense that decorrelation noise is increased [7].

Spectral variance poses problems for strain imaging but also offers opportunities to identify the sources of scattering in biological media. Measurements of Δf_c in breast tissues, for example, may be used to distinguish the relative contribution of scattering from collagen versus lipid structures. If $\Delta f_c = 0$, we can assume lipid acts as a matrix media that contains scatterers but does not itself scatter sound significantly. Alternatively, if $\Delta f_c \simeq 0.1\epsilon'$ for $0 \leq \epsilon' \leq 0.1$ — the maximum strain range for linear elastic behavior in most tissues — then lipid-filled structures are the principal scattering sources, as they were in our oil-in-gel samples. More likely, $\Delta f_c \simeq a\epsilon'$ for $0 \leq \epsilon' \leq 0.1$ and $0 < a < 0.1$. Values of $a > 0.05$ would suggest a dominant role for deformable scatterers.

Given the agreement found between measured and predicted centroid values in Fig 2, we expect a proportional decrease in Δf_c for stretched samples, although those experiments were not performed.

IV. Conclusions

The average sound speed, attenuation, and echo spectrum from random, tissue-like scattering media containing stiff spheres is unchanged by uniaxial compression. This finding verifies a fundamental assumption required for strain imaging using these media. However, the mean echo spectrum increases with compressive strain preferentially at high frequency and in a predictable manner for media containing deformable scatterers. Consequently, the use of ultrasonic echoes to track movement of lipid-filled scattering objects in the body, for example, those in breast tissue, will suffer additional waveform decorrelation in proportion to ϵ'. This effect seen in phantoms has yet to be verified experimentally in tissues. Our results suggest caution in designing strain imaging techniques and new opportunities for identifying scattering sources in biological media.

References

[1] M. Bilgen, M.F. Insana, "Deformation models and correlation analysis in elastography", *J. Acoust. Soc. Am*, Vol. 99, pp. 3212 - 3224, 1996.

[2] S.A. Goss, R.L. Johnston, F. Dunn, "Comprehensive compilation of empirical ultrasonic properties of mammalian tissues II", *J. Acoust. Soc. Am*, Vol. 68, pp. 93 - 108, 1980.

[3] E.L. Madsen, J.A. Zagzebski, G.R. Frank, "Oil-in-gelatin dispersions for use as ultrasonically tissue-mimicking materials", *Ultrasound Med. Biol.*, Vol. 8, pp. 277 - 287, 1982.

[4] T.J. Hall, M. Bilgen, M.F. Insana, T.A. Krouskop, "Phantom materials for elastography", *IEEE Trans. Ultrason. Ferro. Freq. Contrl.*, Vol. 44, pp. 1355–1365, 1997.

[5] R.N. Bracewell, *The Fourier Transform and Its Applications, 2/e*, McGraw-Hill, New York, 1978.

[6] J.J. Bowman, T.B.A. Senior, P.L.E. Uslenghi, "Electromagnetic and Acoustic Scattering by Simple Shapes", North-Holland Publishers, Amsterdam, 1969, Chapter 13.

[7] Y. Zhu, P. Chaturvedi, M.F. Insana, "Strain imaging with a deformable mesh", *Ultrasonic Imaging*, Vol. 21, pp. 127 - 146, 1999.

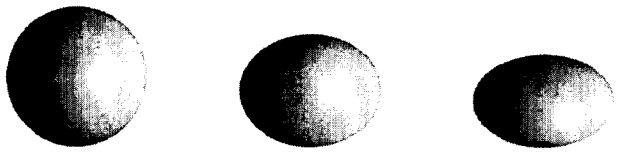

Fig. 3. Oblate spheroids where (l-r) $r(\epsilon') = 0.0, 0.2, 0.4$.

Table 1. Type I Materials: Glass-in-Gel Suspensions.

Sample	Glass Sph Diam	Mass [g/l]	Sound Speed @ 2.5 MHz	Atten Coeff @ 2.5/5.0/7.5/10 MHz
1	35 - 75 μm	33.3	1590 m/s	0.74/1.88/3.83/6.91 dB/cm
2	150 - 180 μm	6.67	1575 m/s	0.47/1.10/1.67/2.71 dB/cm

Table 2. Type II Materials: Oil-in-Gel Dispersions.

Sample	Oil Type Diam	Oil Conc	Sound Speed @ 2.5 MHz	Atten Coeff @ 2.5/5.0/7.5/10 MHz
3, 3'	corn	250 ml/l	1557 m/s (ave)	1.18/3.69/6.90/10.78 dB/cm (ave)
4	motor (SAE 10W30)	250 ml/l	1556 m/s	0.87/3.68/7.56/11.79 dB/cm
5	peanut	250 ml/l	1561 m/s	0.95/3.72/6.85/10.65 dB/cm
6	mineral	250 ml/l	1567 m/s	0.87/2.86/5.03/7.47 dB/cm